

Extreme Tuning of Redox and Optical Properties of Cationic Cyclometalated Iridium(III) Isocyanide Complexes

Nail M. Shavaleev,^{*,†} Filippo Monti,[‡] Rosario Scopelliti,[†] Andrea Baschieri,[§] Letizia Sambri,[§] Nicola Armaroli,^{*,‡} Michael Grätzel,[†] and Mohammad K. Nazeeruddin^{*,†}

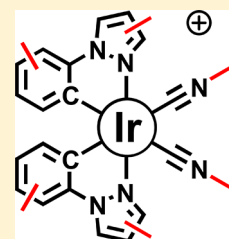
[†]Laboratory of Photonics and Interfaces, École Polytechnique Fédérale de Lausanne, CH-1015 Lausanne, Switzerland

[‡]Molecular Photoscience Group, Istituto per la Sintesi Organica e la Fotoreattività, Consiglio Nazionale delle Ricerche, Via P. Gobetti, 101, 40129, Bologna, Italy

[§]Department of Organic Chemistry "A. Mangini", University of Bologna, Viale Risorgimento 4, 40136, Bologna, Italy

S Supporting Information

ABSTRACT: We report seven heteroleptic cationic iridium(III) complexes with cyclometalating N-arylazoles and alkyl/aryl isocyanides, $[(C^{\wedge}N)_2Ir(CNR)_2](CF_3SO_3)^+$, and characterize two of them by crystal structure analysis. The complexes are air- and moisture-stable white solids that have electronic transitions at very high energy with absorption onset at 320–380 nm. The complexes are difficult to reduce and oxidize; they exhibit irreversible electrochemical processes with peak potentials (against ferrocene) at -2.74 to -2.37 V (reduction) and 0.99 – 1.56 V (oxidation) and have a large redox gap of 3.49 – 4.26 V. The reduction potential of the complex is determined by the azole heterocycle (pyrazole or indazole) and by the isocyanide (*tert*-butyl or 2,6-dimethylphenyl) and the oxidation potential by the Ir–aryl fragment [aryl = 2',4'-R₂-phenyl (R = H/F), 9',9'-dihexyl-2'-fluorenyl]. Three of the complexes exhibit phosphorescence in argon-saturated dichloromethane and acetonitrile solutions at room temperature with 0–0 transitions at 473–478 nm (green color; the emission spectra are solvent-independent), quantum yields of 3–25%, and long excited-state lifetimes of 62–350 μ s. All of the complexes are phosphorescent at 77 K with 0–0 transitions at 387–474 nm (blue to green color). The extremely long calculated radiative lifetimes, 0.5–3.5 ms, confirm that the complexes emit from a cyclometalating-ligand-centered excited state.



INTRODUCTION

We, and others, have recently reported that cationic bis-cyclometalated iridium(III) complexes with 2-phenylpyridines and *tert*-butyl isocyanide, $[(C^{\wedge}N)_2Ir(CNtBu)_2]^+$, exhibit blue/green phosphorescence from a 2-phenylpyridine-centered excited state with high quantum yields (up to 76%), and long excited-state lifetimes (up to 84 μ s) at room temperature.^{1–6} Non-chromophore strong-field electron-withdrawing *tert*-butyl isocyanide ligands⁷ destabilize the excited states, blue-shift the phosphorescence maximum, and enhance the phosphorescence efficiency of these complexes.^{1–6} Phosphorescence of the mono-isocyanide iridium(III) complexes⁸ and of the isocyanide complexes of copper(I),⁹ platinum(II),¹⁰ rhenium(I),^{11–15} and ruthenium(II)^{16–21} has been investigated as well.

Pyridine, a UV chromophore and a strong π -acceptor/ σ -donor, introduces low-energy π - π^* and charge-transfer excited states in metal complexes with polypyridines and cyclometalating arylpyridines.^{22–25} To increase the excited-state energy of a complex, one can replace the pyridine with another metal-binding heterocycle.^{22–32} Here, we report heteroleptic cationic iridium(III) complexes with alkyl/aryl isocyanides and cyclometalating N-arylazoles (1–7, Scheme 1). We tune the redox and optical properties of Ir(III) complexes to the extremes by adjusting the π -conjugation in the ligands and by changing the metal-binding heterocycle. We report the first cyclometalated iridium(III) complexes that are hard to reduce/

oxidize, that are transparent in the visible/near-UV range, and that exhibit phosphorescence with very long radiative lifetimes.

RESULTS AND DISCUSSION

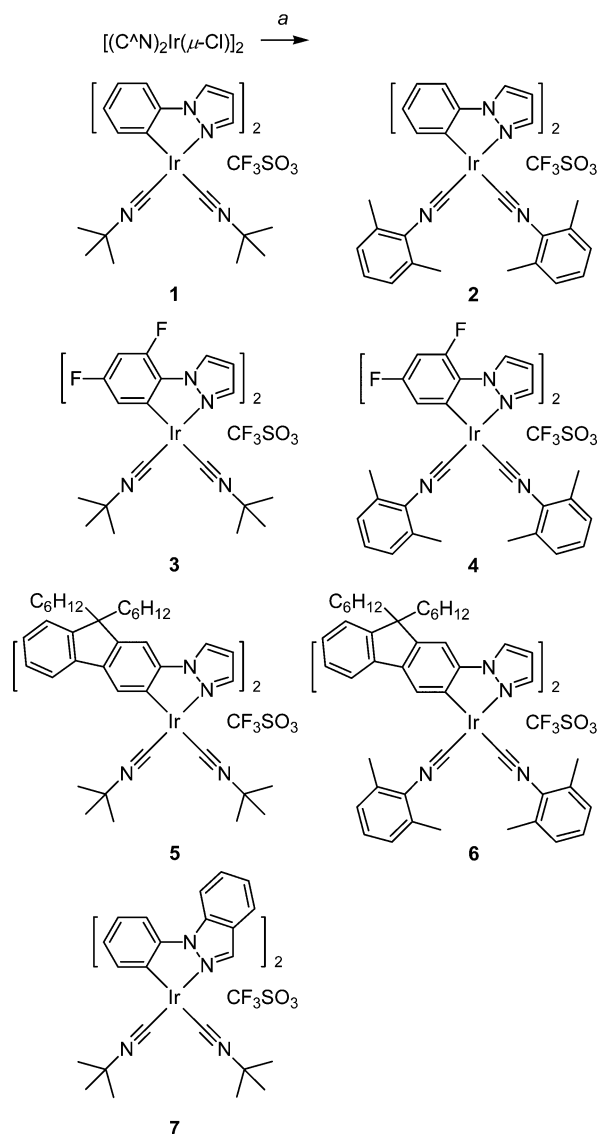
Synthesis. We prepared the new ligand **L** by Cu₂O-catalyzed C–N coupling³³ of 9,9-dihexyl-2-bromofluorene with pyrazole (Scheme 2). The reaction of **L** with IrCl₃·3H₂O in 2-ethoxyethanol/water gave the cyclometalated complex $[(L)_2Ir(\mu-Cl)]_2$ (Scheme 2).

Seven new iridium(III) isocyanide complexes (1–7, Scheme 1) were prepared by the reaction of $[(C^{\wedge}N)_2Ir(\mu-Cl)]_2$ ($C^{\wedge}N$ = N-arylazole)^{31,32,34} with silver triflate (to remove the chloride anion) and with an isocyanide CNR [R = *tert*-butyl (CNtBu), 2,6-dimethylphenyl (CNPh*)].^{1,4–6} Purification by column chromatography on silica and by recrystallization gave 1–7 as air- and moisture-stable white solids that are soluble in polar organic solvents. 1–7 are the first iridium(III) isocyanide complexes with cyclometalating N-arylazoles, and 2, 4, and 6 are the first bis-cyclometalated bis(aryl isocyanide) Ir(III) complexes.^{1–6,8}

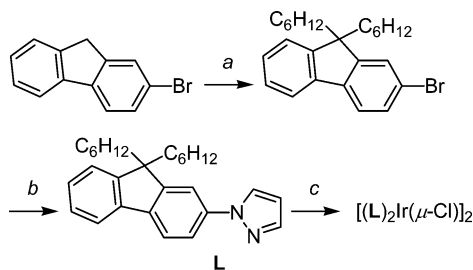
¹H and ¹⁹F NMR spectra of 1–7 (i) exhibit a single set of signals for the C[∧]N and CNR ligands, (ii) confirm the 1:1 ratio of C[∧]N to CNR, (iii) confirm the presence of the F groups and

Received: September 19, 2012

Published: January 9, 2013

Scheme 1. New Iridium(III) Isocyanide Complexes^a

^aReaction conditions: (a) under Ar, room temperature; (i) AgCF_3SO_3 , $\text{CH}_3\text{OH}/\text{CH}_2\text{Cl}_2$; (ii) CNR , CH_2Cl_2 .

Scheme 2. Ligand L and Complex $[(\text{L})_2\text{Ir}(\mu\text{-Cl})]_2$ ^a

^aReaction conditions: (a) bromohexane, KOtBu , dry DMF, under argon, 60 °C; (b) pyrazole, Cs_2CO_3 , Cu_2O (catalyst), dry DMF, under argon, 120 °C; (c) $\text{IrCl}_3 \cdot 3\text{H}_2\text{O}$, 2-ethoxyethanol/water (3/1), under argon, 120 °C.

of the CF_3SO_3^- anion, and (iv) indicate that the complexes have C_2 symmetry. Mass spectra of **1–7** exhibit a peak of the $[(\text{C}^{\wedge}\text{N})_2\text{Ir}(\text{CNR})_2]^+$ cation.

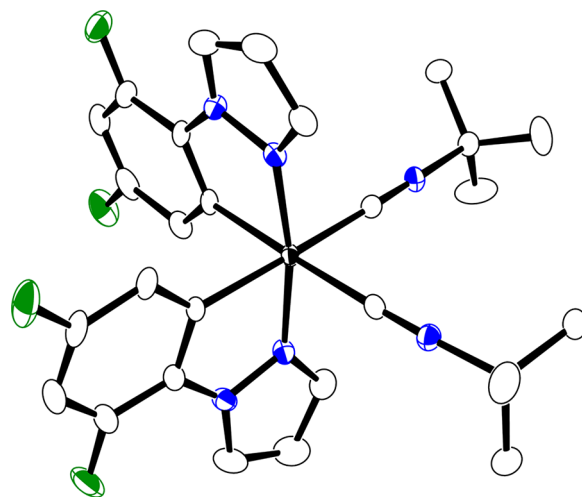
Structures of Ir(III) Isocyanide Complexes. The iridium(III) ion in **3** and **4** (Figures 1 and 2) is in a distorted-

Figure 1. Structure of **3** (50% probability ellipsoids; H atoms and triflate anion omitted; ORTEP). Heteroatoms: N, blue; F, green; Ir, black.

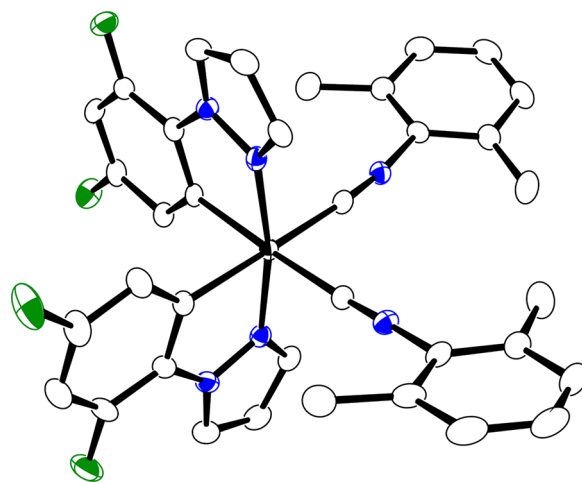


Figure 2. Structure of **4** (50% probability ellipsoids; H atoms and triflate anion omitted; ORTEP). Heteroatoms: N, blue; F, green; Ir, black.

octahedral $[(\text{C}^{\wedge}\text{N})_2\text{Ir}(\text{C})_2]^+$ coordination environment. The two $\text{N}(\text{C}^{\wedge}\text{N})$ atoms are in positions trans to each other. The metal–ligand bond lengths increase in the order $\text{Ir}-\text{C}(\text{CNR}) < \text{Ir}-\text{N}(\text{C}^{\wedge}\text{N}) < \text{Ir}-\text{C}(\text{C}^{\wedge}\text{N})$ (Table 1). The $\text{Ir}-\text{C}$ bonds with CNPh^* (**4**) are shorter than are those with $\text{CN}t\text{Bu}$ (**3**) [the reported $\text{Ir}-\text{CN}t\text{Bu}$ bond lengths in the analogous complexes^{1,4–6} are 2.004(6)–2.062(6) Å]. The Ir –isocyanide fragments, $\text{Ir}-\text{C}\equiv\text{N}$ and $\text{C}\equiv\text{N}-\text{C}$, are not linear (Table 1). The $\text{C}^{\wedge}\text{N}$ ligands are nearly planar with dihedral angles between the phenyl and azole of 1.6–8.9° (Table 1).

Weak face-to-face π – π stacking between the $\text{C}^{\wedge}\text{N}$ ligands in the $\text{CN}t\text{Bu}$ complex **3** gives a dimer structure with an interplanar $\text{C}^{\wedge}\text{N}\cdots\text{C}^{\wedge}\text{N}$ distance of 3.166 Å. Weak face-to-face π – π stacking of the CNPh^* complex **4** gives a chain structure: it involves one of the CNPh^* ligands (centroid \cdots centroid distance between the phenyls 3.650 Å) and one of the $\text{C}^{\wedge}\text{N}$ ligands (interplanar $\text{C}^{\wedge}\text{N}\cdots\text{C}^{\wedge}\text{N}$ distance 3.311 Å). The shortest $\text{Ir}\cdots\text{Ir}$ distance in **3** and **4** exceeds 8 Å.

Table 1. Structural Parameters of Iridium(III) Isocyanide Complexes^a

complex	bond lengths (Å)				bond angles (deg)		
	isocyanide		C [^] N		C [^] N ^b	Ir–C≡N	C≡N–C
	Ir–C	Ir–C	Ir–N	Ir–N			
3	2.026(4)	2.064(3)	2.035(3)	2.031(3)	8.90	178.8(3)	178.6(4)
	2.043(3)	2.057(3)	2.031(3)	2.031(3)	1.90	173.7(3)	173.6(4)
4	2.018(3)	2.069(3)	2.044(2)	2.034(2)	1.60	175.6(2)	172.9(3)
	2.025(3)	2.073(3)	2.034(2)	2.034(2)	6.54	174.7(3)	178.0(3)

^aEach row corresponds to one ligand. The isocyanide ligand is in a position trans to the carbon atom of the C[^]N ligand in the same row. ^bAngle between the aryl and azole rings.

Electrochemistry. We have measured redox potentials of 1–7 (against ferrocene couple) by cyclic voltammetry (CV) in acetonitrile (ACN) and DMF (Figures 3 and 4 and Figures

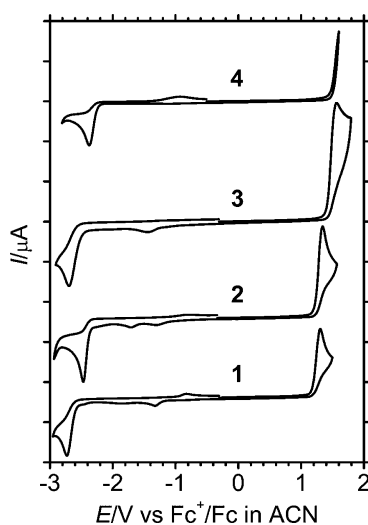


Figure 3. Cyclic voltammograms of 1–4 in acetonitrile (glassy-carbon electrode, 0.1 M NBu₄PF₆, 100 mV/s). The unit on the vertical axis is 50 μA. The peaks at -0.4 to -2.0 V are the return waves of irreversible processes. CVs of 1–4 in DMF are shown in the Supporting Information.

S1–S4 in the Supporting Information). All redox processes were irreversible (Table 2 and Tables S2 and S3 in the Supporting Information). Complexes 1–7 exhibit a reduction at -2.74 to -2.37 V, an oxidation at 0.99–1.56 V, and a redox gap, $\Delta E = E^{\text{ox}} - E^{\text{red}}$, of 3.49–4.26 V (at CV scan rate 100 mV/s; Table 2). Electron-withdrawing 2',4'-fluorines^{25,28,31} increase the redox potentials from 1 and 2 to 3 and 4 by ≤ 130 mV (E^{red}) and ≤ 260 mV (E^{ox}). Changing *tert*-butyl isocyanide (1, 3, 5) to the stronger π -acceptor 2,6-dimethylphenyl isocyanide³⁵ (2, 4, 6) increases the redox potentials by ≤ 330 mV (E^{red}) and ≤ 50 mV (E^{ox}). Replacing a phenyl (1, 2) with a stronger electron-donor fluorenyl (5, 6) facilitates the oxidation by ≤ 310 mV. Replacing a pyrazole (1) with a stronger σ -donor/ π -acceptor indazole³² (7) facilitates both the reduction (by ≤ 360 mV) and the oxidation (by 160 mV).

We find that (i) the redox potentials of 1–7 are nearly solvent-independent in DMF and ACN at a scan rate of 100 mV/s (Table 2), (ii) the redox processes remain irreversible and the trends in redox parameters of 1, 3, 5, and 7 do not change when the scan rate is increased from 100 mV/s to 1 V/s in ACN (Table 2; Figures S2 and S3 and Table S2 in the Supporting Information), and (iii) at scan rates 20–1000 mV/s

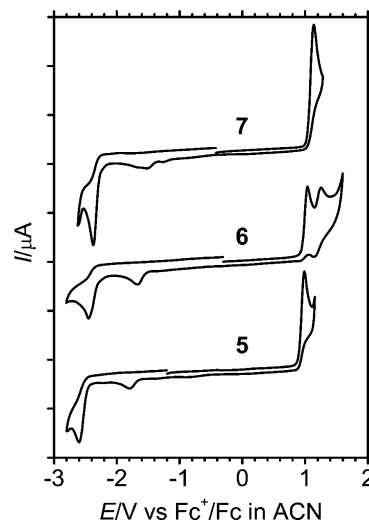


Figure 4. Cyclic voltammograms of 5–7 in acetonitrile (glassy-carbon electrode, 0.1 M NBu₄PF₆, 100 mV/s). The unit on the vertical axis is 20 μA. The peaks at -1.4 to -2.0 V are the return waves of irreversible processes. CVs of 5–7 in DMF are shown in the Supporting Information.

Table 2. Redox Properties^a

complex	CNR ^b	E^{red} , V		E^{ox} , V ^c		ΔE , V ^d	
		DMF	ACN	DMF	ACN	DMF	ACN
1	<i>t</i> Bu	-2.74	-2.73	1.30		4.03	
2	Ph*	-2.50	-2.47	1.34		3.81	
3	<i>t</i> Bu	-2.63	-2.70	1.56		4.26	
4	Ph*	-2.37	-2.37				
5	<i>t</i> Bu	-2.71	-2.60	1.00	0.99	3.71	3.59
6	Ph*	-2.51	-2.45	1.02	1.04	3.53	3.49
7	<i>t</i> Bu	-2.39	-2.37	1.14		3.51	
R ^e	<i>t</i> Bu	-2.38	-2.38	1.23		3.61	

^aIn acetonitrile (ACN) or DMF. All redox processes were irreversible. Oxidation or reduction peak potentials are reported. Relative to Fc⁺/Fc. Estimated errors: ± 50 mV. On glassy-carbon working electrode, in the presence of 0.1 M (NBu₄)PF₆, at scan rate 100 mV/s. ^bSubstituent in the isocyanide ligand. Ph* = 2,6-dimethylphenyl. ^cThe oxidation process was outside of the electrochemical window for 1–4 and 7 in DMF (>1.1 V) and for 4 in ACN (>1.6 V). ^d $\Delta E = E^{\text{ox}} - E^{\text{red}}$. ^eData from the literature. R = [(N,C^{2'}-2-phenylpyridyl)₂Ir(CN*t*Bu)₂](CF₃SO₃)₅.

in ACN, the redox processes of 3 remain irreversible with the peak potentials and gap of -2.66 to -2.78 V (E^{red}), 1.56–1.69 V (E^{ox}), and 4.25–4.40 V (ΔE) (Table S3 and Figure S4 in the Supporting Information).

The redox potentials of 1–7 indicate that the reduction is determined by the azole and isocyanide and the oxidation by the Ir–aryl fragment. The irreversibility of redox processes, which probably arises from a chemical reaction that follows the electron transfer,⁶ prevented us from determining the formal redox potentials; nevertheless, we consider that the peak potentials and the redox gap correctly reproduce the trends in the energies of the HOMO, LUMO, and HOMO–LUMO gap of 1–7.^{5,6,36} The redox gap increases on fluorination from 1 and 2 to 3 and 4 but decreases when *tert*-butyl isocyanide (1, 3, 5) is replaced by 2,6-dimethylphenyl isocyanide (2, 4, 6) and when an aromatic system of the N-arylazole ligand is extended from phenyl or pyrazole (1, 2) to fluorenyl (5, 6) or indazole (7) (Table 2).

Because pyrazole is a weaker π -acceptor/ σ -donor^{22,23,25,28,31} than pyridine, the 1-phenylpyrazole complex 1 in ACN exhibits more negative reduction (by –0.35 V) and more positive oxidation (by 0.07 V) than the reported 2-phenylpyridine analogue **R** does⁵ (Table 2). On the other hand, the reduction potential and π -acceptor strength of 1-phenylindazole (7) are similar to those of 2-phenylpyridine (**R**) (Table 2). The high oxidation potentials of 1–7 arise from the positive charge of the complexes, the strong electron-withdrawing isocyanide ligand, and the weak σ -donor pyrazole.

To summarize, (i) complexes 1–7, especially 1–4, are hard to reduce/oxidize and exhibit a large redox gap, (ii) 3 exhibits the largest redox gap reported for a cyclometalated iridium(III) complex, 4.26 V at 100 mV/s (all of the known Ir(III) complexes with redox gaps >3.5 V exhibit irreversible redox processes^{5,6,31,37}), and (iii) the redox gap of 1–7 is reduced by extending the π -conjugation in the ligands.

Absorption Spectroscopy. The infrared absorption spectra of 1–7 in neat films exhibit two peaks separated by 20–26 cm^{-1} at 2214–2177 cm^{-1} (CN*t*Bu complexes) or 2193–2155 cm^{-1} (CNPh* complexes) that are characteristic of stretching vibrations of the isocyanide C \equiv N bond (Table 3 and Figures S6 and S7 in the Supporting Information).^{5,6} The presence of two IR peaks confirms the *cis* geometry²¹ of the isocyanides in 1–7.

Table 3. UV–Vis and IR Absorption Maxima

	IR, cm^{-1a}	λ_{abs} , nm ($\epsilon/10^3 \text{ M}^{-1} \text{ cm}^{-1}b$)
L		296 (24), 316 (23)
1	2200, 2177	277 (12), 299 (11)
2	2181, 2156	278 (29, sh)
3	2214, 2194	275 (13, sh)
4	2193, 2172	255 (55, sh)
5	2199, 2177	258 (31), 292 (26), 304 (31), 336 (45), 349 (40)
6	2181, 2155	257 (60), 290 (37), 304 (31), 335 (47), 349 (42)
7	2206, 2185	259 (49), 283 (19), 293 (20), 336 (14)

^aInfrared absorption bands of solid films of the neat complex in the region of the C \equiv N stretching vibrations. ^bIn dichloromethane, at room temperature, at 250–600 nm. Estimated errors: ± 2 nm for λ_{abs} ; ± 5 nm for λ_{onset} ; $\pm 5\%$ for ϵ .

Complexes 1–7 are white solids that give colorless solutions in dichloromethane. 1–7 exhibit electronic transitions at very high energy for cyclometalated iridium(III) complexes (Figure 5). We find the following: (i) The wavelength of the absorption onset is determined by the N-arylazole ligand and varies in the order 7 (380 nm) > 5, 6 (370 nm) > 1, 2 (340 nm) > 3, 4 (320 nm) (Figure 5). The shorter wavelength of the absorption

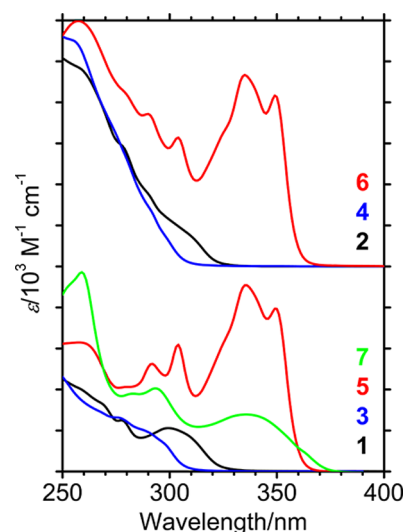


Figure 5. Absorption spectra of 1–7 at $(5.51\text{--}12.3) \times 10^{-5} \text{ M}$ in dichloromethane. The unit on the vertical axis is $10 \times 10^3 \text{ M}^{-1} \text{ cm}^{-1}$.

onset corresponds to the larger redox gap for the complexes with the same isocyanide ligand. (ii) Fluorination of the electron-rich phenyl ring of the C \wedge N ligand blue-shifts the absorption from 1 and 2 to 3 and 4 (Figure 5). (iii) Replacing a phenyl or pyrazole with a stronger electron-donor (fluorenyl) or a stronger electron-acceptor (indazole), respectively, red-shifts and enhances the absorption from 1–4 to 5–7 (we note that fluorenyl and indazole chromophores in 5–7 have lower-energy and higher-intensity π – π^* transitions than pyrazole and phenyl chromophores do in 1–4) (Figure 5). We conclude from i–iii that the lowest energy electronic absorption of the complexes 1–7 is determined by the (Ir–aryl)-to-azole charge-transfer state (CT).^{5,6}

The absorption of 1–7 at 250–300 nm increases by up to $3 \times 10^4 \text{ M}^{-1} \text{ cm}^{-1}$ when *tert*-butyl isocyanide is replaced by the stronger π -acceptor 2,6-dimethylphenyl isocyanide (Figure 5). These new intense high-energy electronic transitions are associated with the (Ir–aryl)-to-CNPh* charge-transfer (CT*).^{8,13,17}

3 and 4 are the first cationic bis-cyclometalated iridium(III) complexes that are transparent in the UV range to 320 nm (Figure 5). The CT and π – π^* absorption transitions of 3 and 4 have high energy because (i) pyrazole is a weak π -acceptor/ σ -donor with high-energy π – π^* transitions,^{22,23,25,28,31} (ii) 2,4-difluorophenyl is a weak electron donor, and (iii) *tert*-butyl and 2,6-dimethylphenyl isocyanides are non-chromophores in the visible and near-UV spectral ranges¹⁷ and are strong electron-withdrawing ligands.

To summarize, the (Ir–aryl)-to-azole charge-transfer state (CT) determines the absorption onset in 1–7; however, we expect the CT state to be mixed with a cyclometalating-ligand-centered (LC) state in 1–7 and with a CT* state in 2 and 4. The absorption onset of 1–7 is red-shifted by extending the π -conjugation in the N-arylazole (but not in the isocyanide).

Phosphorescence Spectroscopy. We have studied the photophysical properties of the complexes 1–7 in dichloromethane (DCM) and acetonitrile (ACN) solutions at room temperature (under argon) and at 77 K (Figure 6 and Table 4; Figure S8 in the Supporting Information). The emission of 1–7 is completely quenched by oxygen at room temperature in liquid solution.

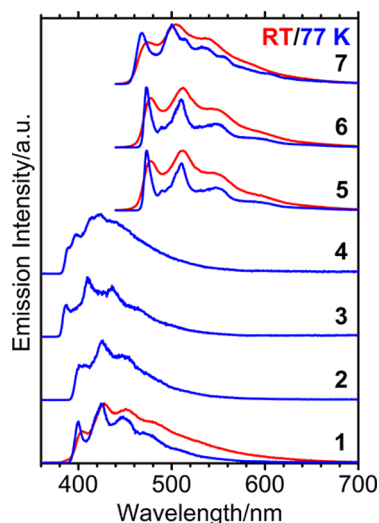


Figure 6. Corrected and normalized luminescence spectra of 1–7 in 10^{-5} M argon-saturated dichloromethane solution at room temperature (red) and at 77 K (blue).

Table 4. Photophysical Properties

complex	medium ^a	λ_{0-0} , nm ^b	λ_{max} , nm ^c	Φ , % ^d	τ , μ s ^e	τ_{rad} , ms ^f
1	DCM	405	428	~0.1		
	77 K	400	425			
2	77 K	406 (br)	426			
3	77 K	387	410			
4	77 K	389 (sh)	424			
	DCM	477	512	8	280	3.5
5	ACN	474	510	3	75	2.5
	77 K	474	474			
	DCM	478	512	10	350	3.5
6	ACN	474	509	3	90	3.0
	77 K	473	473			
	DCM	474	505	25	140	0.5
7	ACN	473	502	8	62	0.8
	77 K	469	500			

^aDichloromethane (DCM) or acetonitrile (ACN) solution at room temperature under argon (10^{-5} M). DCM glass at 77 K. The extreme sensitivity of 5–7 to quenching by trace oxygen/impurities in solutions at room temperature causes a large error of 25% for Φ and τ . ^bHighest energy vibronic luminescence peak (0–0 transition). ^cMaximum of the luminescence spectrum. ^d $\lambda_{exc} = 280$ – 300 nm. $\Phi < 0.1\%$ for 2–4 in DCM at room temperature. ^eThe luminescence decay of 1–4 and 7 in DCM at 77 K is a biexponential function with components of 20–40/140–380 μ s (1–4), 200–250/1100–1300 μ s (5, 6), and 80/390 μ s (7). ^fCalculated radiative lifetime: $\tau_{rad} = \tau/\Phi$.

At room temperature, (i) 1 exhibits blue phosphorescence with 0–0 transition $\lambda_{0-0} = 405$ nm and the quantum yield $\Phi \approx 0.1\%$, (ii) 2–4 are non-emissive with $\Phi < 0.1\%$, and (iii) 5–7 exhibit green phosphorescence with $\lambda_{0-0} = 473$ – 478 nm, $\Phi = 3$ – 25% , observed excited-state lifetime $\tau = 62$ – 350 μ s, and calculated radiative lifetime $\tau_{rad} = \tau/\Phi = 0.5$ – 3.5 ms (Figure 6 and Table 4; Figure S8 in the Supporting Information). The excitation and absorption spectra of the complexes match (Figure S9, Supporting Information). The monoexponential luminescence decays of 5–7 confirm the presence of one emissive center in solution at room temperature (Figure S10, Supporting Information).

The phosphorescence spectra of 5–7 at room temperature are solvent-independent: for example, λ_{0-0} and λ_{max} blue-shift

only by ≤ 4 nm from DCM to ACN. We find that 5–7 exhibit higher Φ and longer τ times in dichloromethane than they do in acetonitrile; however, τ_{rad} in both solvents are similar within experimental error. We consider that acetonitrile (or the trace impurities in it) quenches the extremely long-lived excited states of 5–7 more than dichloromethane does.

At 77 K, the complexes exhibit blue (1–4, $\lambda_{0-0} = 387$ – 406 nm) or green (5–7, $\lambda_{0-0} = 469$ – 474 nm) phosphorescence (Figure 6 and Table 4). The spectra have better resolved vibronic structure at 77 K than they do at room temperature (Figure 6), but λ_{0-0} blue-shifts only by ≤ 5 nm from room temperature to 77 K. The luminescence decays of 1–7 at 77 K are biexponential functions with components of 20–250 μ s and 140–1300 μ s (Figure S11, Supporting Information).

The structured and solvent-independent phosphorescence spectra, together with the long radiative lifetimes, indicate that 1–7 emit from a cyclometalating-ligand-centered excited state (LC) coupled to an (Ir-aryl)-to-azole charge-transfer state (CT).^{5,6,38,39} Replacing CNtBu with CNPh* red-shifts and broadens the emission spectrum from 1 and 3 to 2 and 4 (but not from 5 to 6) because the LC/CT states in 2 and 4 (but not in 6) are close in energy/coupled to the (Ir-aryl)-to-CNPh* charge-transfer state (CT*).

We consider that, at room temperature, the LC/CT state of 1–4 is quenched through thermal population of the proximate non-emissive metal-centered d–d state; hence, $\Phi(1-4) \leq 0.1\%$ (the same non-radiative deactivation mechanism works for the reported Ir(III) complexes with 1-phenylpyrazoles^{26,27,29}). At 77 K, however, 1–4 are phosphorescent and have long excited-state lifetimes because thermally activated quenching is too slow at 77 K to compete with radiative decay.^{26,27,29}

Replacing pyridine with pyrazole increases the redox gap and, therefore, destabilizes the CT state and blue-shifts the phosphorescence spectrum from R ($\lambda_{0-0} = 455$ nm; room temperature, DCM)⁵ to 1 by 50 nm (2700 cm^{-1}). In the same way, fluorination of the C^{^N} ligand further blue-shifts the phosphorescence spectrum from 1 and 2 to 3 and 4 by 13–17 nm (840 – 1080 cm^{-1} ; λ_{0-0} , 77 K). 3 and 4 have the highest energy phosphorescence ($\lambda_{0-0} = 387$ – 389 nm, 77 K) reported for $[(C^{\wedge}N)_2Ir(C)_2]^+$ and $[(C^{\wedge}N)_2Ir(C^{\wedge}C)]^+$ complexes.^{1–6,40,41} Although the quantum yields of 3 and 4 at room temperature are very low, $<0.1\%$, we expect that by replacing a pyrazole with another azole³⁰ one may get efficient high-energy-emitting $[(C^{\wedge}N)_2Ir(CNR)_2]^+$ complexes.

At room temperature, 5–7 have >30 -fold higher emission quantum yields than 1–4 do because the LC/CT states (but not the d–d states) are stabilized (in other words, the energy gap between LC/CT and d–d states increases) when the π conjugation in the N-arylazole ligand is extended from 1–4 to 5–7.

Phosphorescent metal complexes with long excited-state lifetimes are used for singlet oxygen generation^{2,42} and for oxygen sensing.^{4,9,43,44} Because iridium(III) promotes strong spin–orbit coupling, the majority of phosphorescent Ir(III) complexes have relatively short radiative lifetimes: 1–100 μ s.^{38,39,45,46} The rare Ir(III) complexes that do exhibit long radiative lifetime of hundreds to thousands of microseconds are $[(C^{\wedge}N)_2Ir(CNtBu)_2]^+$,^{1–6} $[(C^{\wedge}N)_2Ir(P^{\wedge}P)]^+$ (P[^]P = diphosphine),^{1,46} Ir(III)–corrole,^{47,48} Ir(III)–porphyrin,^{44,48} and $[Ir(1,10\text{-phenanthroline})_3]^3+$.⁴⁹

To our knowledge, 5 and 6 have some of the highest radiative lifetimes of the excited state at room temperature (2.5–3.5 ms) and the highest excited-state lifetimes at 77 K (up

to 1.3 ms) reported for cyclometalated Ir(III) complexes.^{39,45} We consider that, in **5** and **6**, a π -conjugated fluorenyl chromophore stabilizes the LC state, while the weak electron acceptor pyrazole destabilizes the CT state, thereby reducing the LC–CT coupling and increasing both the LC character and the radiative lifetime of the excited state [in iridium(III) complexes, LC states have longer radiative lifetime than CT states do^{38,39,45}].

The radiative lifetime of the complex decreases from **5** and **6** (2.5–3.5 ms) to **7** (0.5–0.8 ms) because the indazole (**7**) stabilizes the CT state and promotes the LC–CT coupling more than the pyrazole does (**5**, **6**) (recall that indazole is a stronger electron acceptor than pyrazole, Table 2). Variation of the isocyanide from **5** (CN*t*Bu) to **6** (CNPh*) does not significantly change the spectrum (λ_{0-0} , λ_{\max}), Φ , τ , or τ_{rad} (Table 4), thereby confirming that the emissive state of the complex is N-arylazole-centered.

The phosphorescence spectra of **1** and **5**, **6** resemble those of the tris-cyclometalated analogues^{24,26,29} [$\text{Ir}(\text{N},\text{C}^{2'}\text{-1-phenylpyrazolyl})_3$] and [$\text{Ir}(\text{N},\text{C}^{3'}\text{-1-(9',9'-dimethyl-2'-fluorenyl)pyrazolyl})_3$], respectively; however, the radiative lifetimes of **5** and **6** (2.5–3.5 ms) are >25-fold higher than that of their [$\text{Ir}(\text{C}^{\wedge}\text{N})_3$] analogue (97²⁴ or 59 μs ²⁹ at room temperature) [we note that enhancement of excited-state lifetime by isocyanide ligands was first reported for Ru(II) complexes¹⁸]. We consider that electron-withdrawing isocyanide ligands strongly destabilize the (Ir–aryl)-to-azole CT state and decouple it from the N-arylazole LC state, thereby increasing the radiative lifetime from [$\text{Ir}(\text{C}^{\wedge}\text{N})_3$] to [$(\text{C}^{\wedge}\text{N})_2\text{Ir}(\text{CNR})_2$]⁺.

Conclusions. Iridium(III) isocyanide complexes with cyclometalating N-arylazoles, [$(\text{C}^{\wedge}\text{N})_2\text{Ir}(\text{CNR})_2$]⁺, exhibit extremely wide redox and optical windows and very long excited-state radiative lifetimes. Facile variation of the N-arylazole and isocyanide ligands opens the way to redox-inert, transparent, and high-energy phosphorescent organometallic iridium(III) complexes.

EXPERIMENTAL SECTION

Purification, crystal growth, and handling of all compounds were carried out under air. All products were stored in the dark. Chemicals from commercial suppliers were used without purification. Chromatography was performed on a column with an i.d. of 30 mm on silica gel 60 (Fluka, No. 60752). The progress of reactions and the elution of products were followed on TLC plates (silica gel 60 F₂₅₄ on aluminum sheets, Merck).

Further experimental details are provided in the Supporting Information.

Synthesis of Ir(III) Isocyanide Complexes 1–7. The structures of **1**–**7** are shown in Scheme 1. The reactions were performed under argon and in the absence of light. The solvents were deoxygenated by bubbling with Ar, but they were not dried. *Caution! tert-Butyl isocyanide is a foul-smelling volatile liquid—ensure adequate ventilation!* [$(\text{C}^{\wedge}\text{N})_2\text{Ir}(\mu\text{-Cl})_2$] was dissolved in CH_2Cl_2 (20 mL) and methanol (5 mL) at room temperature. A solution of AgCF_3SO_3 (excess, Aldrich) in methanol (5 mL) was added dropwise. A precipitate of AgCl immediately formed. The reaction mixture was stirred for 4 h. It was filtered through a paper filter to remove AgCl and evaporated to dryness (these operations were done in air). The resulting Ir(III) bis-solvato complex was suspended in degassed CH_2Cl_2 (15 mL), and isocyanide (excess, Aldrich) was added. The reaction mixture became a solution, and its color changed from yellow to nearly colorless. It was stirred at room temperature under argon for 96 h (for *tert*-butyl isocyanide) or 48–72 h (for 2,6-dimethylphenyl isocyanide) to give a solution. It was directly loaded on the chromatography column (silica, 12 g) to avoid rotavaporating foul-smelling isocyanides. Elution with

0.5% methanol in CH_2Cl_2 removed the impurities. Elution with 1.0–1.5% methanol in CH_2Cl_2 recovered the product as a colorless eluate (brown and blue impurities followed **2** and **4**, respectively, while a yellow impurity preceded **6**; these impurities were easily separated). Purification by chromatography gave the pure product, unless stated otherwise. The complexes were often isolated as oils that solidified on standing. **1**–**6** are non-emissive in the powder form. **7** exhibits weak yellow phosphorescence in the powder form. Further details are provided below.

Complex 1. [$(\text{C}^{\wedge}\text{N})_2\text{Ir}(\mu\text{-Cl})_2$] ($\text{C}^{\wedge}\text{N}$ = 1-phenylpyrazole;³¹ 100 mg, 0.097 mmol), AgCF_3SO_3 (55 mg, 0.214 mmol), and *tert*-butyl isocyanide (0.5 mL, 365 mg, 4.4 mmol) gave a white solid: 114 mg (0.144 mmol, 74%). Anal. Calcd for $\text{C}_{29}\text{H}_{32}\text{F}_3\text{IrN}_6\text{O}_3\text{S}$ (MW 793.88): C, 43.87; H, 4.06; N, 10.59. Found: C, 44.16; H, 4.00; N, 10.29. ¹H NMR (400 MHz, CD_2Cl_2): δ 8.27 (d, J = 2.8 Hz, 2H), 7.92 (d, J = 2.8 Hz, 2H), 7.34 (dd, J = 8.0, 0.8 Hz, 2H), 7.08 (td, J = 8.0, 1.6 Hz, 2H), 6.92–6.82 (m, 4H), 6.19 (dd, J = 7.6, 1.2 Hz, 2H), 1.45 (s, 18H, *tert*-butyl) ppm. ¹⁹F NMR (376 MHz, CD_2Cl_2): δ –78.92 (triflate) ppm. ESI⁺ TOF MS: m/z 645.3 ($\{\text{M} - \text{CF}_3\text{SO}_3\}^+$, 100%).

Complex 2. [$(\text{C}^{\wedge}\text{N})_2\text{Ir}(\mu\text{-Cl})_2$] ($\text{C}^{\wedge}\text{N}$ = 1-phenylpyrazole;³¹ 100 mg, 0.097 mmol) in CH_2Cl_2 (10 mL) AgCF_3SO_3 (58 mg, 0.226 mmol), and 2,6-dimethylphenyl isocyanide (195 mg, 1.49 mmol) gave a white solid: 155 mg (0.174 mmol, 90%). Anal. Calcd for $\text{C}_{37}\text{H}_{32}\text{F}_3\text{IrN}_6\text{O}_3\text{S}$ (MW 889.97): C, 49.93; H, 3.62; N, 9.44. Found: C, 50.66; H, 3.65; N, 8.90. ¹H NMR (400 MHz, CD_2Cl_2): δ 8.32 (d, J = 3.2 Hz, 2H), 8.09 (d, J = 2.4 Hz, 2H), 7.41 (dd, J = 8.0, 0.8 Hz, 2H), 7.28 (t, J = 7.6 Hz, 2H), 7.19–7.11 (m, 6H), 6.95 (td, J = 7.6, 0.8 Hz, 2H), 6.87 (t, J = 2.4 Hz, 2H), 6.35 (dd, J = 7.6, 1.2 Hz, 2H), 2.18 (s, 12H, CH_3) ppm. ¹⁹F NMR (376 MHz, CD_2Cl_2): δ –78.98 (3F, triflate) ppm. ESI⁺ TOF MS: m/z 741.2 ($\{\text{M} - \text{CF}_3\text{SO}_3\}^+$, 100%).

Complex 3. [$(\text{C}^{\wedge}\text{N})_2\text{Ir}(\mu\text{-Cl})_2$] ($\text{C}^{\wedge}\text{N}$ = 1-(2',4'-difluorophenyl)pyrazole;³¹ 100 mg, 0.085 mmol), AgCF_3SO_3 (48 mg, 0.187 mmol), and *tert*-butyl isocyanide (0.5 mL, 365 mg, 4.4 mmol) gave a white solid: 119 mg (0.137 mmol, 81%). Anal. Calcd for $\text{C}_{29}\text{H}_{28}\text{F}_7\text{IrN}_6\text{O}_3\text{S}$ (MW 865.84): C, 40.23; H, 3.26; N, 9.71. Found: C, 41.33; H, 3.45; N, 9.32. ¹H NMR (400 MHz, CD_2Cl_2): δ 8.49 (d, J = 2.8 Hz, 2H), 7.93 (d, J = 2.4 Hz, 2H), 6.88 (t, J = 2.8 Hz, 2H), 6.74–6.65 (m, 2H), 5.68–5.61 (m, 2H), 1.49 (s, 18H, *tert*-butyl) ppm. ¹⁹F NMR (376 MHz, CD_2Cl_2): δ –78.89 (3F, triflate), –112.05 (d, $J_{\text{F-F}}$ = 6 Hz, 2F), –123.95 (d, $J_{\text{F-F}}$ = 6 Hz, 2F) ppm. ESI⁺ TOF MS: m/z 717.2 ($\{\text{M} - \text{CF}_3\text{SO}_3\}^+$, 100%).

Complex 4. The reaction was performed with [$(\text{C}^{\wedge}\text{N})_2\text{Ir}(\mu\text{-Cl})_2$] ($\text{C}^{\wedge}\text{N}$ = 1-(2',4'-difluorophenyl)pyrazole;³¹ 100 mg, 0.085 mmol), AgCF_3SO_3 (48 mg, 0.187 mmol), and 2,6-dimethylphenyl isocyanide (200 mg, 1.52 mmol). After chromatography, the product still contained impurities; therefore, it was recrystallized. It was dissolved in CH_2Cl_2 (3 mL) and poured into ether (30 mL) with stirring. The product was filtered and washed with ether to give a white solid: 116 mg (0.121 mmol, 71%). Anal. Calcd for $\text{C}_{37}\text{H}_{28}\text{F}_7\text{IrN}_6\text{O}_3\text{S}$ (MW 961.93): C, 46.20; H, 2.93; N, 8.74. Found: C, 46.28; H, 2.67; N, 8.46. ¹H NMR (400 MHz, CD_2Cl_2): δ 8.56 (d, J = 3.2 Hz, 2H), 8.14 (d, J = 2.4 Hz, 2H), 7.32 (t, J = 7.6 Hz, 2H), 7.19 (d, J = 7.6 Hz, 4H), 6.92 (t, J = 2.8 Hz, 2H), 6.81–6.72 (m, 2H), 5.87–5.81 (m, 2H), 2.23 (s, 12H, CH_3) ppm. ¹⁹F NMR (376 MHz, CD_2Cl_2): δ –78.98 (3F, triflate), –111.38 (d, $J_{\text{F-F}}$ = 6 Hz, 2F), –123.43 (d, $J_{\text{F-F}}$ = 6 Hz, 2F) ppm. ESI⁺ TOF MS: m/z 813.2 ($\{\text{M} - \text{CF}_3\text{SO}_3\}^+$, 100%).

Complex 5. [$(\text{L})_2\text{Ir}(\mu\text{-Cl})_2$] (Supporting Information; 100 mg, 0.049 mmol), AgCF_3SO_3 (28 mg, 0.11 mmol), and *tert*-butyl isocyanide (0.25 mL, 183 mg, 2.2 mmol) gave a white solid: 121 mg (0.093 mmol, 94%). Anal. Calcd for $\text{C}_{67}\text{H}_{88}\text{F}_3\text{IrN}_6\text{O}_3\text{S}$ (MW 1306.73): C, 61.58; H, 6.79; N, 6.43. Found: C, 61.64; H, 6.87; N, 6.17. ¹H NMR (400 MHz, CD_2Cl_2): δ 8.38 (d, J = 2.8 Hz, 2H), 7.98 (d, J = 2.0 Hz, 2H), 7.45–7.38 (m, 2H), 7.34 (s, 2H), 7.33–7.26 (m, 2H), 7.27–7.21 (m, 4H), 6.97–6.92 (m, 2H), 6.60 (s, 2H), 2.02–1.92 (m, 4H), 1.93–1.83 (m, 4H), 1.37 (s, 18H, *tert*-butyl), 1.14–0.85 (m, 24H), 0.76 (t, J = 7.2 Hz, 6H), 0.64 (t, J = 6.8 Hz, 6H), 0.68–0.58 (m, 4H), 0.51–0.41 (m, 4H) ppm. ¹⁹F NMR (376 MHz, CD_2Cl_2): δ –78.9 (3F, triflate) ppm. ESI⁺ TOF MS: m/z 1157.67 ($\{\text{M} - \text{CF}_3\text{SO}_3\}^+$, 100%).

Complex 6. $[(L)_2Ir(\mu-Cl)]_2$ (Supporting Information; 100 mg, 0.049 mmol), $AgCF_3SO_3$ (30 mg, 0.117 mmol), and 2,6-dimethylphenyl isocyanide (148 mg, 1.13 mmol) gave a white solid: 109 mg (0.078 mmol, 79%). Anal. Calcd for $C_{75}H_{88}F_3IrN_6O_3S$ (MW 1402.82): C, 64.21; H, 6.32; N, 5.99. Found: C, 64.47; H, 6.28; N, 5.76. 1H NMR (400 MHz, CD_2Cl_2): δ 8.44 (d, $J = 1.2$ Hz, 2H), 8.17 (d, $J = 2.4$ Hz, 2H), 7.45–7.39 (m, 4H), 7.34–7.21 (m, 8H), 7.10 (d, $J = 7.6$ Hz, 4H), 6.97 (t, $J = 2.4$ Hz, 2H), 6.74 (s, 2H), 2.15 (s, 12H, CH_3), 2.04–1.94 (m, 4H), 1.94–1.84 (m, 4H), 1.15–0.85 (m, 24H), 0.76 (t, $J = 7.2$ Hz, 6H), 0.64 (t, $J = 6.8$ Hz, 6H), 0.69–0.59 (m, 4H), 0.57–0.45 (m, 4H) ppm. ^{19}F NMR (376 MHz, CD_2Cl_2): δ –78.96 (3F, triflate) ppm. ESI⁺ TOF MS: m/z 1253.7 ($\{M - CF_3SO_3\}^+$, 100%).

Complex 7. $[(C^{\wedge}N)_2Ir(\mu-Cl)]_2$ ($C^{\wedge}N = 1$ -phenylindazole; 32 90 mg, 0.073 mmol), $AgCF_3SO_3$ (42 mg, 0.163 mmol), and *tert*-butyl isocyanide (0.35 mL, 255 mg, 3.1 mmol) gave a white solid: 112 mg (0.125 mmol, 86%). Anal. Calcd for $C_{37}H_{36}F_3IrN_6O_3S$ (MW 894.00): C, 49.71; H, 4.06; N, 9.40. Found: C, 50.13; H, 4.04; N, 9.08. 1H NMR (400 MHz, CD_2Cl_2): δ 8.57 (s, 2H), 8.33 (d, $J = 8.8$ Hz, 2H), 8.10 (d, $J = 8.0$ Hz, 2H), 7.90 (d, $J = 8.0$ Hz, 2H), 7.81–7.74 (m, 2H), 7.56 (t, $J = 7.6$ Hz, 2H), 7.18–7.11 (m, 2H), 6.76 (td, $J = 7.6, 0.8$ Hz, 2H), 6.11 (dd, $J = 7.6, 1.2$ Hz, 2H), 1.45 (s, 18H, *tert*-butyl). ^{19}F NMR (376 MHz, CD_2Cl_2): δ –78.9 (3F, triflate). ESI⁺ TOF MS: m/z 745.26 ($\{M - CF_3SO_3\}^+$, 100%).

■ ASSOCIATED CONTENT

■ Supporting Information

Experimental techniques; synthesis of 9,9-dihexyl-2-bromo-fluorene, ligand L, and complex $[(L)_2Ir(\mu-Cl)]_2$; crystallographic data (Table S1); cyclic voltammograms (Tables S2 and S3; Figures S1–S4); absorption spectra (Figures S5–S7); emission spectra (Figure S8); excitation spectra (Figure S9); luminescence decays (Figures S10 and S11); NMR spectra; CIF of the crystal structures of 3 and 4, CCDC 909628 and 909629. This material is available free of charge via the Internet at <http://pubs.acs.org>.

■ AUTHOR INFORMATION

■ Corresponding Author

*Tel: +41 21 693 6124. Fax: +41 21 693 4111. E-mail: nail.shavaleev@epfl.ch (N.M.S.); nicola.armoroli@cnr.it (N.A.); mdkhaja.nazeeruddin@epfl.ch (M.K.N.).

■ Notes

The authors declare no competing financial interest.

■ ACKNOWLEDGMENTS

Financial support was given by the European Union (CELLO, STRP 248043; <https://www.cello-project.eu/>) and the CNR (MACOL, PM.P04.010).

■ REFERENCES

- Li, J.; Djurovich, P. I.; Alleyne, B. D.; Yousufuddin, M.; Ho, N. N.; Thomas, J. C.; Peters, J. C.; Bau, R.; Thompson, M. E. *Inorg. Chem.* **2005**, *44*, 1713.
- Abdel-Shafi, A. A.; Bourdelande, J. L.; Ali, S. S. *Dalton Trans.* **2007**, 2510.
- Wang, X.; Li, J.; Thompson, M. E.; Zink, J. I. *J. Phys. Chem. A* **2007**, *111*, 3256.
- Habibagahi, A.; Mebarki, Y.; Sultan, Y.; Yap, G. P. A.; Crutchley, R. J. *ACS Appl. Mater. Interfaces* **2009**, *1*, 1785.
- Shavaleev, N. M.; Monti, F.; Costa, R.; Scopelliti, R.; Bolink, H. J.; Ortí, E.; Accorsi, G.; Armaroli, N.; Baranoff, E.; Grätzel, M.; Nazeeruddin, Md. K. *Inorg. Chem.* **2012**, *51*, 2263.
- Shavaleev, N. M.; Monti, F.; Scopelliti, R.; Armaroli, N.; Grätzel, M.; Nazeeruddin, Md. K. *Organometallics* **2012**, *31*, 6288.
- Kuznetsov, M. L. *Russ. Chem. Rev.* **2002**, *71*, 265.

(8) Dedeian, K.; Shi, J.; Forsythe, E.; Morton, D. C.; Zavalij, P. Y. *Inorg. Chem.* **2007**, *46*, 1603.

- Smith, C. S.; Mann, K. R. *J. Am. Chem. Soc.* **2012**, *134*, 8786.
- Lai, S.-W.; Lam, H.-W.; Lu, W.; Cheung, K.-K.; Che, C.-M. *Organometallics* **2002**, *21*, 226.
- Sacksteder, L.; Lee, M.; Demas, J. N.; DeGraff, B. A. *J. Am. Chem. Soc.* **1993**, *115*, 8230.
- Stoyanov, S. R.; Villegas, J. M.; Cruz, A. J.; Lockyear, L. L.; Reibenspies, J. H.; Rillema, D. P. *J. Chem. Theory Comput.* **2005**, *1*, 95.
- Villegas, J. M.; Stoyanov, S. R.; Reibenspies, J. H.; Rillema, D. P. *Organometallics* **2005**, *24*, 395.
- Villegas, J. M.; Stoyanov, S. R.; Huang, W.; Rillema, D. P. *Inorg. Chem.* **2005**, *44*, 2297.
- (a) Ng, C.-O.; Lo, L. T.-L.; Ng, S.-M.; Ko, C.-C.; Zhu, N. *Inorg. Chem.* **2008**, *47*, 7447. (b) Ko, C.-C.; Siu, J. W.-K.; Cheung, A. W.-Y.; Yiu, S.-M. *Organometallics* **2011**, *30*, 2701.
- Connor, J. A.; Meyer, T. J.; Sullivan, B. P. *Inorg. Chem.* **1979**, *18*, 1388.
- Larowe, J. E.; McMillin, D. R.; Stacy, N. E.; Tetrack, S. M.; Walton, R. A. *Inorg. Chem.* **1987**, *26*, 966.
- Indelli, M. T.; Bignozzi, C. A.; Marconi, A.; Scandola, F. *J. Am. Chem. Soc.* **1988**, *110*, 7381.
- Myrick, M. L.; De Armond, M. K. *J. Phys. Chem.* **1989**, *93*, 7099.
- Villegas, J. M.; Stoyanov, S. R.; Huang, W.; Lockyear, L. L.; Reibenspies, J. H.; Rillema, D. P. *Inorg. Chem.* **2004**, *43*, 6383.
- Leung, C.-F.; Ng, S.-M.; Xiang, J.; Wong, W.-Y.; Lam, M. H.-W.; Ko, C.-C.; Lau, T.-C. *Organometallics* **2009**, *28*, 5709.
- Jameson, D. L.; Blaho, J. K.; Kruger, K. T.; Goldsby, K. A. *Inorg. Chem.* **1989**, *28*, 4312.
- Ayers, T.; Scott, S.; Goins, J.; Caylor, N.; Hathcock, D.; Slattery, S. J.; Jameson, D. L. *Inorg. Chim. Acta* **2000**, *307*, 7.
- Sajoto, T.; Djurovich, P. I.; Tamayo, A.; Yousufuddin, M.; Bau, R.; Thompson, M. E.; Holmes, R. J.; Forrest, S. R. *Inorg. Chem.* **2005**, *44*, 7992.
- Tamayo, A. B.; Garon, S.; Sajoto, T.; Djurovich, P. I.; Tsyba, I. M.; Bau, R.; Thompson, M. E. *Inorg. Chem.* **2005**, *44*, 8723.
- Karatsu, T.; Ito, E.; Yagai, S.; Kitamura, A. *Chem. Phys. Lett.* **2006**, *424*, 353.
- (a) Treboux, G.; Mizukami, J.; Yabe, M.; Nakamura, S. *Chem. Lett.* **2007**, *36*, 1344. (b) Yang, L.; Okuda, F.; Kobayashi, K.; Nozaki, K.; Tanabe, Y.; Ishii, Y.; Haga, M.-a. *Inorg. Chem.* **2008**, *47*, 7154.
- He, L.; Duan, L.; Qiao, J.; Wang, R.; Wei, P.; Wang, L.; Qiu, Y. *Adv. Funct. Mater.* **2008**, *18*, 2123.
- Sajoto, T.; Djurovich, P. I.; Tamayo, A. B.; Oxgaard, J.; Goddard, W. A., III; Thompson, M. E. *J. Am. Chem. Soc.* **2009**, *131*, 9813.
- (a) Mydlak, M.; Bizzarri, C.; Hartmann, D.; Sarfert, W.; Schmid, G.; De Cola, L. *Adv. Funct. Mater.* **2010**, *20*, 1812. (b) Costa, R. D.; Ortí, E.; Bolink, H. J.; Graber, S.; Housecroft, C. E.; Constable, E. C. *J. Am. Chem. Soc.* **2010**, *132*, 5978. (c) Sykes, D.; Tidmarsh, I. S.; Barbieri, A.; Sazanovich, I. V.; Weinstein, J. A.; Ward, M. D. *Inorg. Chem.* **2011**, *50*, 11323. (d) Ladouceur, S.; Fortin, D.; Zysman-Colman, E. *Inorg. Chem.* **2011**, *50*, 11514.
- Shavaleev, N. M.; Scopelliti, R.; Baranoff, E.; Grätzel, M.; Nazeeruddin, Md. K. *Inorg. Chim. Acta* **2012**, *383*, 316.
- Shavaleev, N. M.; Scopelliti, R.; Grätzel, M.; Nazeeruddin, Md. K. *Inorg. Chim. Acta* **2012**, *388*, 84.
- Correa, A.; Bolm, C. *Adv. Synth. Catal.* **2007**, *349*, 2673.
- (a) Nonoyama, M. *J. Organomet. Chem.* **1975**, *86*, 263. (b) Sprouse, S.; King, K. A.; Spellane, P. J.; Watts, R. J. *J. Am. Chem. Soc.* **1984**, *106*, 6647.
- Treichel, P. M.; Dirreen, G. E.; Mueh, H. J. *J. Organomet. Chem.* **1972**, *44*, 339.
- Cardona, C. M.; Li, W.; Kaifer, A. E.; Stockdale, D.; Bazan, G. C. *Adv. Mater.* **2011**, *23*, 2367.
- (a) Yang, C.-H.; Li, S.-W.; Chi, Y.; Cheng, Y.-M.; Yeh, Y.-S.; Chou, P.-T.; Lee, G.-H.; Wang, C.-H.; Shu, C.-F. *Inorg. Chem.* **2005**, *44*, 7770. (b) Song, Y.-H.; Chiu, Y.-C.; Chi, Y.; Cheng, Y.-M.; Lai, C.-

H.; Chou, P.-T.; Wong, K.-T.; Tsai, M.-H.; Wu, C.-C. *Chem. Eur. J.* **2008**, *14*, 5423.

(38) Colombo, M. G.; Hauser, A.; Güdel, H. *Inorg. Chem.* **1993**, *32*, 3088.

(39) Flamigni, L.; Barbieri, A.; Sabatini, C.; Ventura, B.; Barigelletti, F. *Top. Curr. Chem.* **2007**, *281*, 143.

(40) Chin, C. S.; Eum, M.-S.; Kim, S. y.; Kim, C.; Kang, S. K. *Eur. J. Inorg. Chem.* **2007**, 372.

(41) Yang, C.-H.; Beltran, J.; Lemaure, V.; Cornil, J.; Hartmann, D.; Sarfert, W.; Fröhlich, R.; Bizzarri, C.; De Cola, L. *Inorg. Chem.* **2010**, *49*, 9891.

(42) Djurovich, P. I.; Murphy, D.; Thompson, M. E.; Hernandez, B.; Gao, R.; Hunt, P. L.; Selke, M. *Dalton Trans.* **2007**, 3763.

(43) (a) Bacon, J. R.; Demas, J. N. *Anal. Chem.* **1987**, *59*, 2780. (b) Demas, J. N.; DeGraff, B. A.; Coleman, P. B. *Anal. Chem.* **1999**, *71*, 793A. (c) Huo, C.; Zhang, H.; Zhang, H.; Zhang, H.; Yang, B.; Zhang, P.; Wang, Y. *Inorg. Chem.* **2006**, *45*, 4735. (d) Borisov, S. M.; Nuss, G.; Haas, W.; Saf, R.; Schmuck, M.; Klimant, I. *J. Photochem. Photobiol. A: Chem.* **2009**, *201*, 128.

(44) (a) Koren, K.; Borisov, S. M.; Saf, R.; Klimant, I. *Eur. J. Inorg. Chem.* **2011**, 1531. (b) Koren, K.; Dmitriev, R. I.; Borisov, S. M.; Papkovsky, D. B.; Klimant, I. *ChemBioChem* **2012**, *13*, 1184.

(45) (a) Dixon, I. M.; Collin, J.-P.; Sauvage, J.-P.; Flamigni, L.; Encinas, S.; Barigelletti, F. *Chem. Soc. Rev.* **2000**, *29*, 385. (b) Williams, J. A. G.; Wilkinson, A. J.; Whittle, V. L. *Dalton Trans.* **2008**, 2081. (c) You, Y.; Park, S. Y. *Dalton Trans.* **2009**, 1267. (d) Ulbricht, C.; Beyer, B.; Friebe, C.; Winter, A.; Schubert, U. S. *Adv. Mater.* **2009**, *21*, 4418. (e) Hu, T.; He, L.; Duan, L.; Qiu, Y. *J. Mater. Chem.* **2012**, *22*, 4206. (f) Costa, R. D.; Orti, E.; Bolink, H. J.; Monti, F.; Accorsi, G.; Armaroli, N. *Angew. Chem., Int. Ed.* **2012**, *51*, 8178.

(46) Lowry, M. S.; Hudson, W. R.; Pascal, R. A., Jr.; Bernhard, S. *J. Am. Chem. Soc.* **2004**, *126*, 14129.

(47) Palmer, J. H.; Durrell, A. C.; Gross, Z.; Winkler, J. R.; Gray, H. B. *J. Am. Chem. Soc.* **2010**, *132*, 9230.

(48) Palmer, J. H.; Brock-Nannestad, T.; Mahammed, A.; Durrell, A. C.; VanderVelde, D.; Virgil, S.; Gross, Z.; Gray, H. B. *Angew. Chem., Int. Ed.* **2011**, *50*, 9433.

(49) Ayala, N. P.; Flynn, C. M., Jr.; Sacksteder, L.; Demas, J. N.; DeGraff, B. A. *J. Am. Chem. Soc.* **1990**, *112*, 3837.